Slot Die Coating of CIGS Nanoparticle Inks for Scalable Solution Processed Photovoltaics

Ryan G. Ellis[1], Doojin Vak[2], Anthony S. R. Chesman[2], and Rakesh Agrawal[1]

[1]Purdue University – Davidson School of Chemical Engineering, West Lafayette, Indiana, 47901, USA
[2]CSIRO – Manufacturing, Clayton, Victoria, 3168, Australia

***Abstract* — Cu(In,Ga)(S,Se)$_2$ photovoltaics are an attractive absorber material that have demonstrated high efficiencies in excess of 22% using vacuum processes. In order to further reduce production costs, high throughput, high materials utilization, and solution based fabrication techniques such as slot die coating must be realized. In this work a wide variety of coating parameters were explored to enable high quality, uniform, and crack free coatings of Cu(In,Ga)S$_2$ nanoparticle inks via slot die coating under ambient conditions. Slot die coated films were selenized and completed into full devices yielding active area efficiencies up to 11.7%, demonstrating the feasibility of the technique for large scale manufacturing.**

***Index Terms* — coatings, nanoparticles, photovoltaic cells, thin films.**

I. Introduction

Cu(In,Ga)(S,Se)$_2$ (CIGSSe) photovoltaics have emerged as a commercially viable thin film material with long term stability and power conversion efficiencies up to 22.9% [1]. However, current high efficiency devices are fabricated using three stage coevaporation or sputtered metallic precursor layers. These vacuum processes suffer from low materials utilization and low throughput. Solution processing is an attractive alternative fabrication method which has the potential to significantly reduce manufacturing costs through atmospheric pressure processing and high throughput roll-to-roll compatibility. However, high throughput coating techniques are relatively absent in the solution processed CIGSSe literature. A large amount of laboratory scale solution processing of CIGSSe photovoltaics is performed using non roll-to-roll compatible coating techniques such as spin coating, which has very poor materials utilization. Table 1 details a wide variety of solution processed CIGSSe devices and their fabrication methods.

Power conversion efficiencies up to 18.1% have been demonstrated using a hydrazine based molecular precursor approach using spin coating [2]. However, hydrazine is extremely toxic and explosive posing significant challenges for scale up. Spray coating, while roll-to-roll compatible, is known for poor film quality and lower materials utilization. Currently, a colloidal nanocrystal ink using hexanethiol as a solvent has reached the highest non-hydrazine solution processed efficiency of 15% using blade coating [3]. Roll-to-roll compatible inkjet analogues of this system have yielded low power conversion efficiencies of only 6.5% [4]. In this work we adapt the colloidal nanoparticle approach for use with the scalable coating technique, slot die coating. Slot die coating offers high throughput with virtually 100% materials utilization. A custom built 3D printer based lab scale slot die coater was used to screen a wide variety of ink compositions and coating conditions [8]. Optimized coatings were developed using a chlorobenzene/dichlorobenzene solvent mixture. Devices were fabricated from such coatings yielding active area efficiencies up to 11.7% (10.7% total area). To the best of our knowledge, this is the first report of slot die coated CIGSSe absorber layers demonstrating a path to low-cost large scale fabrication of CIGSSe photovoltaics.

TABLE I
Overview of various solution processed CIGSSe solar cells and their deposition method

Power Conversion Efficiency (%)	Solvent System	Deposition Method	Reference
18.1%	Hydrazine	Spin Coating	[2]
13.12%	Thiol-Amine	Spin Coating	[5]
10.5%	Aqueous	Spray Pyrolysis	[6]
14.7%	DMSO	Spin Coating	[7]
15.0%	Hexanethiol	Blade Coating	[3]
6.5%	Hexanethiol/ Dodecanethiol	Inkjet Printing	[4]

II. Experimental

Cu(In,Ga)S$_2$ nanoparticles were fabricated as described in a previous report [3]. Nanoparticles were purified using three successive suspension and precipitation cycles with hexane, isopropyl alcohol, and centrifugation. The nanoparticles were then dried under argon flow and suspended in toluene, chlorobenzene (CB), 1,2-dichlorobenzene (DCB), or a 1:1 vol:vol mixture of CB and DCB. Prior to coating, the ink was filtered through a 1 μm syringe filter. Coating was performed using a batch slot die coater fabricated from a modified 3D printer. Details of the fabrication and use of the slot die coater are described in a previous report [8]. The substrate temperature was varied between room temperature and 65°C during coatings. For all trials, the slot die gap, ink

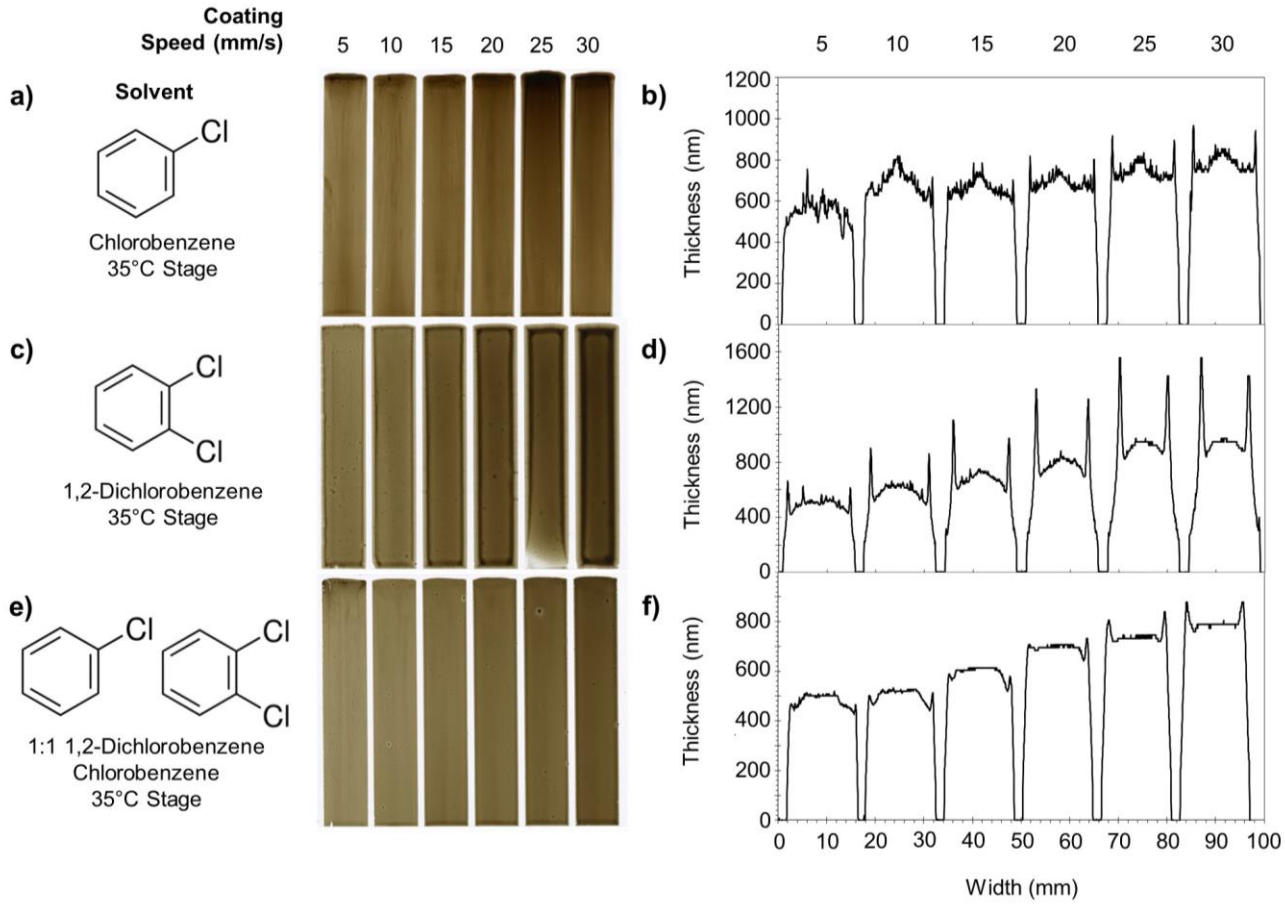

Fig. 1. Color scans and generated width profiles from CIGS nanoparticle inks with various solvents. a) Color scans of chlorobezene ink films and b) their generated thickness profiles across the width. c) Color scans of 1,2-dichlorobenzene ink films and d) their generated thickness profiles across the width. e) Color scans of chlorobenzene/1,2-dichlorobenzene cosolvent ink films and f) their generated thickness profiles across the width.

concentration and dispense rate were set at 100 µm, 250 mg/mL, and 1µL/cm^2 respectively. Absorbance measurements were taken using EPSON Perfection V600 and V700 scanners in transmission mode at 700 dpi. Devices were fabricated on soda lime glass substrates coated with 800 nm of molybdenum via sputtering. The CIGS ink was slot die coated in 13 mm wide stripes. Sodium doping was supplied by electron beam evaporation of ~22.5 nm of NaF. Nanoparticle films were cut to ~1/2" x 1" samples and annealed under an argon/selenium atmosphere at 500°C for 15-25 minutes (selenized). Devices were finished with 50 nm of CdS by chemical bath deposition. ZnO (80 nm) and ITO (220 nm) were deposited via sputtering. Finally Ni (100 nm) and Al (1.5 µm) grids were deposited by E-beam evaporation. Devices were isolated using mechanical scribing with a cell area of 0.47 cm^2 and tested under AM 1.5 simulated light.

III. Results and Discussion

The tested inks wet clean soda-lime glass and molybdenum similarly, thus initial coatings were performed on transparent glass substrates to enable optical absorption measurements in transmission mode using a commercial photo film scanner. Absorbance was correlated to thickness using scribed step height measurements from a Dektak 6M Stylus Profilometer to generate a calibration curve. The as-synthesized particles contained ~8 wt% oleylamine as a surface ligand as determined by TGA and quantitative ^{1}H-NMR measurements. As such, colloidal stability was observed in non-polar solvents with dielectric constants ranging from ~2-10. Toluene, chlorobenzene, and dichlorobenzene were screened as solvents. Conventional slot die coating is considered a pre-metered process in which the coating thickness is set by the ink dispense rate. However, the small scale lab coater operates in a hybrid of pre-metered and self-metered regimes whereby there is some film thickness dependence on both ink flow rate and coating parameters such as coating speed and substrate temperature. As such, various substrate temperatures and coatings speeds were iterated for each solvent system. Toluene was quickly observed to poorly suspend the particles over the time scale of an hour resulting in nanoparticle settling in the syringe pump. This caused time variant coatings, and toluene

was not considered further. CB and DCB were observed to provide significantly more stable colloidal suspensions. Fig. 1 shows color scans of several coatings using CB, DCB, and a 1:1 mixture of each along with thickness profiles generated from absorbance images along the width. The CB coatings appeared significantly more matte as opposed to the high shine of DCB coatings. This was attributed to small aggregate formation in the ink due to the nanoparticles' lower colloidal stability in CB as compared to DCB. This resulted in significant surface roughness, as can be seen in Fig. 1 b). The surface roughness was accompanied by streak like structures along the length of the film. DCB yielded the best colloidal stability of the tested solvents, however, a "coffee ring" like pattern was observed on the edges of each coating, increasing in prevalence for thicker films. Additionally, the surface between the "coffee ring" features became arc shaped. The coffee ring pattern and arced surface are apparent in the width profile as shown in Fig. 1 d). The emergence of these "coffee ring" patterns were correlated with the speed at which the wet film dried, with the tallest coffee ring features appearing in the thickest and thereby slowest drying films. Although the CB films exhibited significant surface roughness, the "coffee ring" feature was much less pronounced. As such, a 1:1 vol:vol co-solvent mixture of CB and DCB was prepared to induce faster drying while maintaining some of the superior colloidal stability of DCB. Fig. 1 e) shows the color scan of the film with markedly less coffee ring. The surface roughness of a chlorobenzene ink was also suppressed using the co-solvent method as shown in the width profile in Fig. 1 f). A three dimensional reconstruction of the films using absorbance measurements shows improved width and length uniformity of the coatings using the co-solvent ink as shown in Fig. 2.

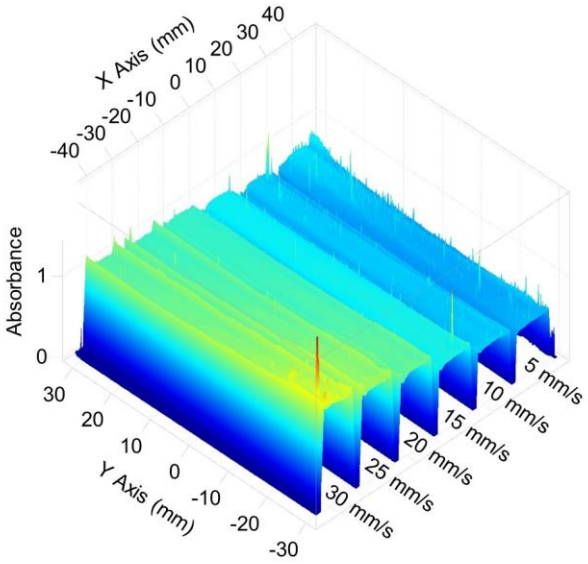

Fig. 2. 3D film reconstruction via absorbance scanning showing minimal "coffee ring" and increased width and length uniformity using the CB/DCB co-solvent

When coated as sequential stripes, superb length uniformity could be obtained after the first stripe.

The optimized co-solvent ink conditions were transferred to molybdenum substrates to enable device fabrication. Films on molybdenum substrates were coated from a single coating pass at 30 mm/s and a 35°C stage temperature yielding a ~830 nm thick nanoparticle film. Residual solvent was removed using a two-step annealing procedure under ambient conditions followed by natural cooling yielding largely crack free films as shown in Fig. 3.

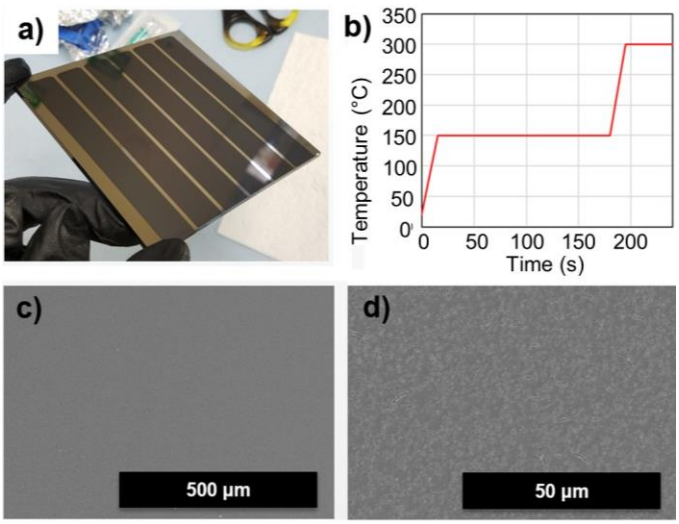

Fig. 3. **a)** An image of a molybdenum coated substrate with stripes of CIGS nanoparticles **b)** A representative annealing profile to prevent cracking **c) / d)** SEM micrographs of the nanoparticle film surfaces showing largely microcrack free films

Devices were finished as described in the experimental section. Full films were cut and small area cells were isolated using mechanical scribing yielding a device area of 0.47 cm^2 A finished device cross section and J-V curve is shown in Fig. 4 and Fig. 5 respectively. Active area efficiencies of up to 11.7% were achieved without the use of an antireflective coating, demonstrating the feasibility of the slot die coating technique for the fabrication of CIGSSe absorber layers.

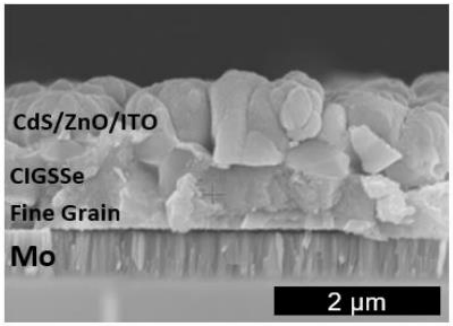

Fig. 4. SEM cross-section of champion device

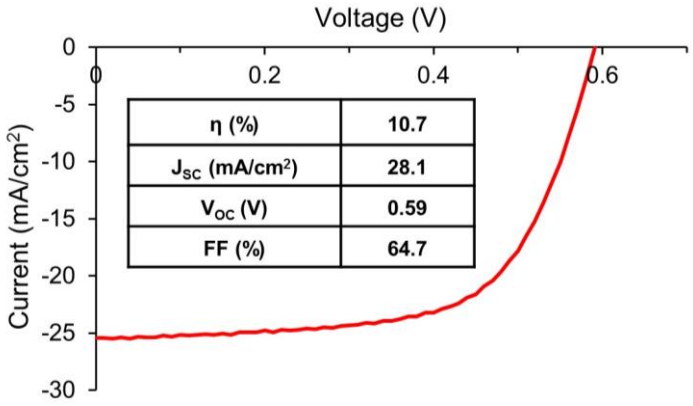

Fig. 5. J-V sweep for the champion device with a total area efficiency of 10.7%

IV. Conclusions

A wide variety of coating conditions were explored to obtain uniform thin films of CIGS nanoparticles using slot die coating. It was found 1,2-dichlorobenzene exhibited the best colloidal stability of the solvents tested, but the high boiling point and slow drying caused a "coffee ring" pattern to appear on the films. Adding a lower boiling co-solvent, chlorobenzene, suppressed the formation of "coffee rings" while maintaining the good colloidal stability of DCB. Through gentle solvent removal, virtually crack free films of nanoparticles could be obtained at thicknesses approaching a micron in a single coating pass. Devices fabricated from these films showed active area efficiencies up to 11.7% demonstrating the feasibility of slot die coating for the fabrication of CIGSSe absorber layers.

Acknowledgements

This work was supported by the NSF through the NRT program under award 1735282 and funding from the Australian Centre for Advanced Photovoltaics (ACAP). The authors would also like to acknowledge Essam AlRuqobah, David Rokke, and Swapnil Deshmukh for their assistance in preparing nanoparticles as well as Joseph Andler, and Xianyi Hu for preparing Mo coated soda lime glass substrates.

References

[1] Solar Frontier, "Solar Frontier Achieves World Record Thin-Film Solar Cell Efficiency of 22.9%," *December 20th*, 2017. [Online]. Available: http://www.solar-frontier.com/eng/news/2017/1220_press.html. [Accessed: 15-Jan-2019].

[2] T. Zhang, Y. Yang, D. Liu, S. C. Tse, W. Cao, Z. Feng, S. Chen, and L. Qian, "High efficiency solution-processed thin-film Cu(In,Ga)(Se,S)$_2$ solar cells," *Energy Environ. Sci.*, vol. 9, no. 12, pp. 3674–3681, 2016.

[3] S. M. McLeod, C. J. Hages, N. J. Carter, and R. Agrawal, "Synthesis and characterization of 15% efficient CIGSSe solar cells from nanoparticle inks," *Prog. Photovoltaics Res. Appl.*, vol. 23, no. 11, pp. 1550–1556, 2015.

[4] J. Barbé, J. Eid, E. Ahlswede, S. Spiering, M. Powalla, R. Agrawal, and S. Del Gobbo, "Inkjet printed Cu(In,Ga)S$_2$ nanoparticles for low-cost solar cells," *J. Nanoparticle Res.*, vol. 18, no. 12, p. 379, 2016.

[5] Q. Fan, Q. Tian, H. Wang, F. Zhao, J. Kong, and S. Wu, "Regulating the starting location of front-gradient enabled highly efficient Cu(In,Ga)Se $_2$ solar cells *via* a facile thiol–amine solution approach," *J. Mater. Chem. A*, vol. 6, no. 9, pp. 4095–4101, 2018.

[6] M. A. Hossain, Z. Tianliang, L. K. Keat, L. Xianglin, R. R. Prabhakar, S. K. Batabyal, S. G. Mhaisalkar, and L. H. Wong, "Synthesis of Cu(In,Ga)(S,Se)$_2$ thin films using an aqueous spray-pyrolysis approach, and their solar cell efficiency of 10.5%," *J. Mater. Chem. A*, vol. 3, no. 8, pp. 4147–4154, 2015.

[7] A. R. Uhl, J. K. Katahara, and H. W. Hillhouse, "Molecular-ink route to 13.0% efficient low-bandgap CuIn(S,Se)$_2$ and 14.7% efficient Cu(In,Ga)(S,Se)$_2$ solar cells," *Energy Environ. Sci.*, vol. 9, no. 1, pp. 130–134, 2016.

[8] D. Vak, K. Hwang, A. Faulks, Y. S. Jung, N. Clark, D. Y. Kim, G. J. Wilson, and S. E. Watkins, "3D printer based slot-die coater as a lab-to-fab translation tool for solution-processed solar cells," *Adv. Energy Mater.*, vol. 5, no. 4, 2015.